Structural Regions of the Cardiac Ca Channel α_{1C} Subunit Involved in Ca-dependent Inactivation

Brett Adams* and Tsutomu Tanabe‡

From the *Department of Physiology and Biophysics, University of Iowa, Iowa City, Iowa, 52242; and ‡Department of Cellular and Molecular Physiology, and Howard Hughes Medical Institute, Yale University School of Medicine, New Haven, Connecticut 06536

ABSTRACT We investigated the molecular basis for Ca-dependent inactivation of the cardiac L-type Ca channel. Transfection of HEK293 cells with the wild-type α_{1C} or its 3′ deletion mutant ($\alpha_{1C-3'del}$) produced channels that exhibited prominent Ca-dependent inactivation. To identify structural regions of α_{1C} involved in this process, we analyzed chimeric α_1 subunits in which one of the major intracellular domains of α_{1C} was replaced by the corresponding region from the skeletal muscle α_{1S} subunit (which lacks Ca-dependent inactivation). Replacing the NH_2 terminus or the III–IV loop of α_{1C} with its counterpart from α_{1S} had no appreciable effect on Ca channel inactivation. In contrast, replacing the I–II loop of α_{1C} with the corresponding region from α_{1S} dramatically slowed the inactivation of Ba currents while preserving Ca-dependent inactivation. A similar but less pronounced result was obtained with a II–III loop chimera. These results suggest that the I–II and II–III loops of α_{1C} may participate in the mechanism of Ca-dependent inactivation. Replacing the final 80% of the COOH terminus of α_{1C} with the corresponding region from α_{1S} completely eliminated Ca-dependent inactivation without affecting inactivation of Ba currents. Significantly, Ca-dependent inactivation was restored to this chimera by deleting a nonconserved, 211–amino acid segment from the end of the COOH terminus. These results suggest that the distal COOH terminus of α_{1S} can block Ca-dependent inactivation, possibly by interacting with other proteins or other regions of the Ca channel. Our findings suggest that structural determinants of Ca-dependent inactivation are distributed among several major cytoplasmic domains of α_{1C}.

KEY WORDS: α_{1S} • skeletal muscle • L-type Ca channel • chimeric proteins • heart

INTRODUCTION

L-type Ca channels perform essential roles in the cardiovascular system, where they trigger excitation–contraction coupling and contribute to pacemaker and action potentials (Boyett et al., 1996). Inactivation of L-type channels is induced by membrane depolarization and elevations in intracellular [Ca], although these two types of Ca channel inactivation appear to proceed via distinct and independent mechanisms (Hadley and Lederer, 1991; Obejero-Paz et al., 1991; Shirokov et al., 1993). Ca-dependent inactivation is a prominent feature of cardiac L-type Ca channels that has important implications for the function of these channels in cardiovascular physiology.

Voltage-gated Ca channels are heteromultimeric complexes composed of pore-forming α_1 and accessory $\alpha_2\delta$ and β subunits (Hofmann et al., 1994). Transfection of mammalian cell lines or *Xenopus* oocytes with the cardiac α_1 subunit (α_{1C}) by itself produces voltage-gated Ca channels that exhibit Ca-dependent inactivation (Neely et al., 1994; Perez-Garcia et al., 1995; Zong and Hofmann, 1996), suggesting that this type of inactivation is an intrinsic property of the α_{1C} subunit. Because Ca-dependent inactivation is induced by a rise in intracellular Ca concentration (Haack and Rosenberg, 1994), it is reasonable to postulate that cytoplasmic domains of α_{1C} participate in its molecular mechanism. The five major putative cytoplasmic domains of α_{1C} include the NH_2 and COOH termini and three linkers (the I–II, II–III, and III–IV loops) that connect the four major transmembrane domains (Mikami et al., 1989).

Two previous studies have provided evidence that one or more of these cytoplasmic domains play important roles in Ca-dependent inactivation. Thus, Ca-dependent inactivation is abolished by simultaneous replacement of all five of the major cytoplasmic domains of α_{1C} with the corresponding regions from the skeletal muscle α_{1S} subunit (Zong et al., 1994). Ca-dependent inactivation is also eliminated by replacing all or a portion of the COOH terminus of α_{1C} with the corresponding region of the neuronal α_{1E} subunit (de Leon et al., 1995). Because α_{1S} and α_{1E} both appear to exhibit only voltage-dependent inactivation (Donaldson and Beam, 1983; Beam and Knudson, 1988; de Leon et al., 1995), these results imply that the structural determinants of

Dr. Tanabe's present address is Department of Pharmacology, Tokyo Medical and Dental University, School of Medicine, Tokyo 113, Japan

Address correspondence to Dr. Brett Adams, Department of Physiology and Biophysics, University of Iowa, Iowa City, IA, 52242. Fax: 319-335-7330; E-mail: brett-adams@uiowa.edu

Ca-dependent inactivation are encoded within the cytoplasmic domains of α_{1C}. The goal of the present study was to test this hypothesis. Toward this end, we have studied a series of chimeric α_1 subunits in which the major cytoplasmic domains of α_{1C} were individually replaced by their counterpart from α_{1S}. Our results suggest that the cytoplasmic COOH terminus, and I–II and II–III loops are all involved in the molecular mechanism of Ca-dependent inactivation. In addition, our findings indicate that Ca-dependent inactivation can be prevented by the distal COOH terminus from the skeletal muscle α_{1S}. Some of these results have appeared previously in abstract form (Adams and Tanabe, 1996).

MATERIALS AND METHODS

Cell Culture and Transfection

Human embryonic kidney cells were obtained from the American Type Culture Collection (CRL 1573; Rockville, MD) and propagated using standard techniques. The culture medium contained 90% DMEM (11995-065; GIBCO BRL, Gaithersburg, MD), 10% heat-inactivated horse serum (26050-13; GIBCO BRL) and 50 μg/ml gentamicin (15710-015; GIBCO BRL). Every 2–3 d, these cells were briefly trypsinized and replated onto the maintenance culture at a fourfold lower density. At the time of replating, additional 35-mm culture dishes (3001; Becton Dickinson & Co., Franklin Lakes, NJ) were seeded with $\sim 10^3$ cells/dish. Approximately 16 h later, the $CaPO_4$ precipitation technique (Cell Phect Kit; Pharmacia LKB Biotechnology Inc., Piscataway, NJ) was used to transfect the seeded cells with a combination (at 1 μg of each plasmid cDNA per dish) of expression plasmids encoding the rabbit cardiac α_{1C} (or chimeras constructed between α_{1C} and the rabbit α_{1S}) and the rabbit skeletal muscle $\alpha_2\delta_a$ and β_{1a} subunits. The transfection mixture also included an expression plasmid (EBO-pCD-Leu2; 59565; American Type Culture Collection) encoding the human CD8 protein at a fivefold lower concentration (0.2 μg per dish). 1–3 d later, paramagnetic beads (4.5 μm diameter) coated with anti–CD8 antibody (Dynal, Inc., Great Neck, NY) were added to each dish. Cells expressing CD8 protein on the surface membrane were visually identified by virtue of being decorated with the beads (Jurman et al., 1994) and were selected for electrophysiological analysis.

Molecular Biology

The amino acid compositions and construction of the expression plasmids encoding the 3′ deletion mutant of α_{1C} ($\alpha_{1C-3'del}$) and the chimeric α_1 subunits CSk1, CSk2, CSk3, and CSk4 have been previously described (Tanabe et al., 1990*b*; Zong et al., 1994). The cDNAs encoding the chimeras CSk5 and CSk8 are composed of the following restriction fragments (the origin of the fragments is given in parentheses). pCSk5: 4.2-kb pair HindIII-AatII (pCARD1; see Mikami et al., 1989), 0.88-kb pair AatII-BglII (pCARD1), and 0.55-kb pair BglII-HindIII (pC6Δ1; see Beam et al., 1992). pCSk8: 3.8-kb pair HindIII-BspHI (pCARD1), 0.24-kb pair BspHI-BstXI (pCAC6; see Tanabe et al., 1988), 0.19-kb pair BstXI-AatII (pCARD1), and 2.9-kb pair AatII-HindIII (pCARD1). The expression plasmids pCSk5 and pCSk8, carrying the cDNAs encoding the individual chimeric Ca channels, were constructed by inserting the corresponding cDNAs into the HindIII site of the plasmid pKCRH2 (Mishina et al., 1984).

The amino acid compositions of CSk5 and CSk8 are as follows (C and Sk, cardiac and skeletal muscle Ca channel, respectively; numbers in parentheses, amino-acid numbers [Tanabe et al., 1987; Mikami et al., 1989]; the junctional sequences common to the two Ca channels are represented by amino acid numbers of the cardiac Ca channel). CSk5: C (1–1634) and Sk (1510–1662). CSk8: C (1–1204), Sk (1074–1129), and C (1261–2171).

Electrophysiology

Patch pipettes were fabricated from 100-μl borosilicate micropipettes (53432-921; VWR Scientific, West Chester, PA) and filled with a solution containing (mM): 155 CsCl, 10 Cs_2EGTA, 4 MgATP, 0.38 Tris-GTP, and 10 HEPES, with pH adjusted to 7.4 using CsOH. Aliquots of this solution were stored at −80°C and kept on ice after thawing. The internal solution was filtered (0.22 μm) immediately before use. Filled pipettes had DC resistances of 1–2 MΩ. Pipette tips were coated with paraffin to reduce capacitance, and then fire polished. Residual pipette capacitance was compensated in the cell-attached configuration, using the negative capacitance circuit of the Axopatch 200A amplifier (Axon Instruments, Inc., Foster City, CA). In earlier experiments, the external solution contained (mM): 145 tetraethylammonium (TEA)[1] chloride, 40 $CaCl_2$ or $BaCl_2$, and 10 HEPES, with pH adjusted to 7.4 using TEAOH. In later experiments, an external solution containing (mM) 140 NaCl, 2 KCl, 40 $CaCl_2$ or $BaCl_2$, and 10 HEPES (pH 7.4 with NaOH or HCl) was used because the cells appeared to remain healthy for longer periods in this solution. Because the voltage dependence of ionic currents recorded in the NaCl-based solution was shifted by −10 mV relative to currents recorded in the TEACl-based solution, data obtained using the two different external solutions have been analyzed separately. Experiments were performed at room temperature (20–23°C). Voltages reported in this paper have not been corrected for liquid junction potentials.

Ca or Ba currents were recorded using the whole-cell patch-clamp technique (Hamill et al., 1981). After establishment of the whole-cell configuration, electronic compensation was used to minimize the access resistance and the time required to charge the cell capacitance. The DC resistance of the whole-cell configuration typically exceeded 1 GΩ, and leakage currents were usually <50 pA at the steady holding potential of −80 mV. Linear cell capacitance was monitored throughout each experiment and was calculated from the integral of charges required to clamp the membrane from −80 to −70 mV. The compensated series resistance (R_S) was calculated from the time constant for decay of the capacity transient and the linear cell capacitance. Depolarizing test pulses were delivered at 5-s intervals. Linear membrane capacitance and leakage currents were subtracted from test currents using the −P/6 method, and all analyzed and reported data were obtained from corrected currents. Currents were filtered at 0.5–10 kHz using the built-in Bessel filter (4-pole low pass) of the Axopatch 200A patch-clamp amplifier, and were sampled at 1–50 kHz using a Digidata 1200 analogue-to-digital board installed in a Gateway 486-66V personal computer. The pCLAMP software programs Clampex and Clampfit (version 6.0) were used for data acquisition and analysis, respectively. Figures were made using Origin (version 4.1).

RESULTS

Fig. 1 shows whole-cell Ca or Ba currents recorded from a human embryonic kidney cell expressing the

[1]*Abbreviations used in this paper:* R_S, compensated series resistance; TEA, tetraethylammonium.

wild-type α_{1C} subunits. As demonstrated by previous studies (Perez-Reyes et al., 1994; Zong et al., 1994; de Leon et al., 1995; Perez-Garcia et al., 1995; Ferreira et al., 1997), the heterologously expressed cardiac α_{1C} exhibits prominent Ca-dependent inactivation, as evidenced by the faster inactivation of Ca than Ba currents. The inactivation rate of currents mediated by the subunit combination expressed here (α_{1C}, $\alpha_2\delta_a$, and β_{1a}) closely approximates the inactivation rate of natively expressed cardiac channels (see Imredy and Yue, 1994), and is considerably faster than the inactivation rate of currents mediated by expression of α_{1C} and β_{2a} in the absence of $\alpha_2\delta_a$ (Perez-Reyes et al., 1994; de Leon et al., 1995; Perez-Garcia et al., 1995; Ferreira et al., 1997).

To quantify the time course of inactivation, the decaying phase of Ca or Ba currents was fit with a single or double exponential function. Most Ca currents required two exponentials for a good fit, whereas Ba currents evoked by relatively short test pulses (250 ms) could usually be well fit by a single exponential. However, some Ba currents displayed two distinct components of inactivation. Fig. 1 *D* plots the time constants for inactivation of α_{1C} currents as a function of test potential. For Ca currents, the time constants for inactivation had a U-shaped dependence on test potential, whereas time constants for inactivation of Ba currents decreased progressively with increasing test potential. These results are consistent with the expectation that α_{1C} undergoes Ca- but not Ba-dependent inactivation. However, in some cells the availability of Ba currents (measured using a double-pulse protocol) displayed a weak U-shaped dependence on test potential (data not shown), consistent with the idea that Ba can also trigger ion-dependent inactivation, although less effectively than Ca.

To investigate the structural basis for Ca-dependent inactivation, we expressed a series of chimeric α_1 subunits in which one of the major intracellular domains of α_{1C} was replaced by the corresponding region from the skeletal muscle α_{1S} subunit. The composition of these chimeras is represented diagrammatically in Fig. 2.

Previous studies have shown that deletion of the distal COOH terminus of α_{1C} or α_{1S} produces a fully functional Ca channel (Beam et al., 1992; Zong et al., 1994; de Leon et al., 1995). Fig. 3 *A* confirms this result for the deletion mutant $\alpha_{1C-3'del}$ in which amino acids 1813–2166 have been removed from the COOH terminus of α_{1C}. As shown in Table I, inactivation of $\alpha_{1C-3'del}$ proceeded at the same rate as the wild-type α_{1C}, confirming that deletion of the distal COOH terminus of α_{1C} does not appreciably alter the process of Ca-dependent inactivation.

We next examined the potential role of the NH_2 terminus in Ca-dependent inactivation. The NH_2 terminus of α_{1C} is 103 amino acids longer than that of α_{1S} (Mikami et al., 1989) and contains four consensus sites for potential phosphorylation by PKC, whereas the NH_2 terminus of α_{1S} lacks predicted PKC sites. In chimera CSk1, the NH_2 terminus of α_{1C} has been replaced by its counterpart from α_{1S} (Fig. 2). Currents mediated by CSk1 closely resembled those produced by α_{1C} and $\alpha_{1C-3'del}$ (Fig. 3 *B*). Thus, Ca currents inactivated faster than Ba currents, and time constants for inactivation of Ca currents were indistinguishable between CSk1 and α_{1C} (Table I). However, inactivation of Ba currents was

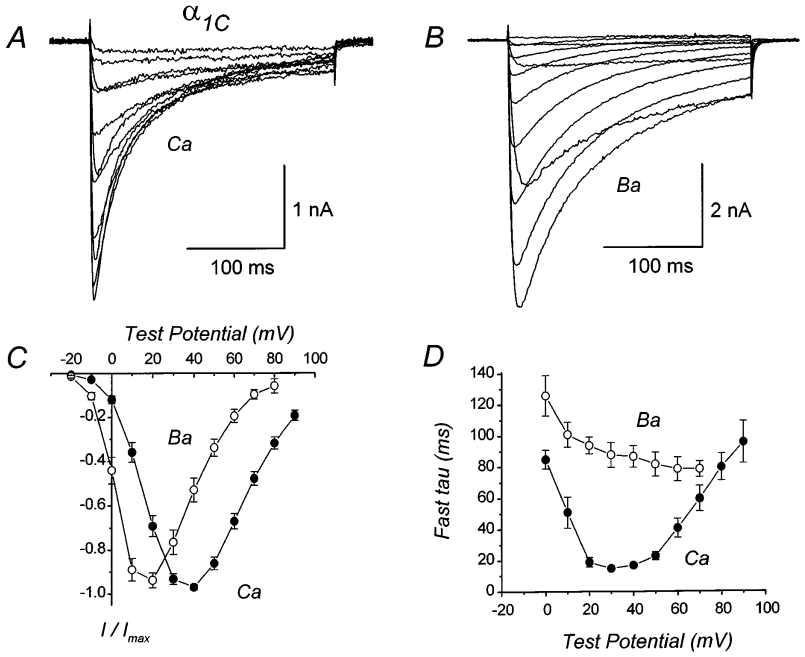

FIGURE 1. Ca-dependent inactivation of wild-type α_{1C} Ca channels coexpressed in HEK293 cells with skeletal muscle $\alpha_2\delta_a$ and β_{1a} subunits. (*A*) Representative whole-cell Ca currents mediated by α_{1C}. The illustrated currents were evoked by depolarizations from −10 to +90 mV. The compensated series resistance (R_S) was 4.2 MΩ. Linear cell capacitance (C) = 41 pF. File 96506016. (*B*) Representative Ba currents mediated by α_{1C}. Test pulses −20 to +90 mV. Same cell as in *A*. R_S = 2.1 MΩ. File 96506018. (*C*) Average *I–V* relations for Ca and Ba currents mediated by α_{1C}. Each plotted point represents the mean (±SEM) of 13 (Ca) and 6 (Ba) different cells. (*D*) Time constants for inactivation of Ca or Ba currents mediated by α_{1C}. Currents were evoked by 250-ms test pulses and were fit with either a single or double exponential function. For currents requiring two exponentials, only the fastest component was included in the analysis. Each plotted point represents the mean (±SEM) of 2–14 (Ca) and 3–7 (Ba) different cells. Experiments summarized in this figure were done using the TEACl-based external solution.

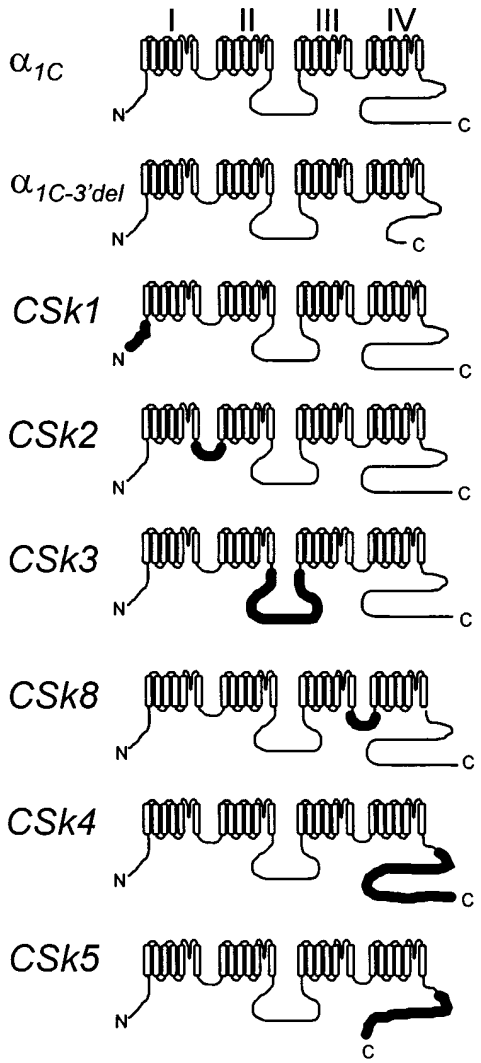

FIGURE 2. Schematic representations of the expressed α_1 subunits. Thinner lines denote regions having amino acid sequence corresponding to the rabbit cardiac α_{1C} subunit (Mikami et al., 1989); thicker lines denote regions corresponding to the rabbit skeletal muscle α_{1S} subunit (Tanabe et al., 1987). The amino acid composition of $\alpha_{1C-3'del}$ and construction of its cDNA has been previously described; the final five amino acid residues from the COOH terminus of α_{1C} (GVSSL) are retained in $\alpha_{1C-3'del}$ (Zong et al., 1994). The amino acid composition and cDNA construction of CSk1, CSk2, CSk3, and CSk4 are described in Tanabe et al. (1990*b*). The compositions of CSk5 and CSk8 and the constructions of their cDNAs are described in MATERIALS AND METHODS.

slightly faster for CSk1 than for α_{1C}. Overall, these results suggest that Ca-dependent inactivation was not significantly altered by replacing the NH_2 terminus of α_{1C} with the corresponding region from α_{1S}.

The Ca channel α_1 subunit is highly homologous to the α subunit of voltage-gated Na channels, and the cytoplasmic linker between transmembrane domains III and IV (the III–IV loop) of Na channels is a critical structural determinant of fast inactivation (Vassilev et al., 1988; Stühmer et al., 1989). To examine the possibility that the homologous III–IV loop of Ca channels is involved in Ca-dependent inactivation, we constructed chimera CSk8 in which the III–IV loop and the first half of IVS1 of α_{1C} were replaced by the corresponding region from α_{1S} (Fig. 2). As shown in Fig. 3 *C*, Ca currents mediated by CSk8 inactivated faster than Ba currents and in general closely resembled currents produced by expression of $\alpha_{1C-3'del}$ or CSk1. Furthermore, the time constants for inactivation of currents mediated by CSk8 were comparable to those obtained for α_{1C}, $\alpha_{1C-3'del}$, and CSk1 (Table I), suggesting that Ca-dependent inactivation is not altered in CSk8.

In both α_{1C} and α_{1S}, the I–II loop contains a number of negatively charged aspartate and glutamate residues that could potentially form a Ca-coordination site or sites. There are 25 negatively charged residues within the I–II loop of α_{1C} and 19 such residues within the I–II loop of α_{1S}. To examine the possibility that the extra acidic residues within the I–II loop of α_{1C} might play a functional role in Ca-dependent inactivation, we expressed chimera CSk2 in which the I–II loop and most of the IIS1 segment of α_{1C} were replaced by the corresponding region from α_{1S} (Fig. 2).

Fig. 4 *A* presents Ca and Ba currents mediated by CSk2. For comparison, currents recorded under identical conditions from cells expressing α_{1C} are shown in Fig. 4 *B*. Ca currents produced by CSk2 inactivated significantly faster than Ba currents, indicating the presence of Ca-dependent inactivation. Furthermore, when relatively long test pulses (1.25 s) were used, both Ca and Ba currents exhibited two distinct components of inactivation. As recently shown by Ferreira et al. (1997) for α_{1C}, the fast component of Ba current inactivation likely represents an ion-dependent process because it parallels Ba influx, whereas the slow component of inactivation likely represents a voltage-dependent process because it parallels the immobilization of gating charge. The presence of two components for inactivation of currents mediated by CSk2 is consistent with the thesis of Ferreira et al. (1997) that Ba as well as Ca can trigger inactivation. In the present work, we have analyzed only the faster time constants for inactivation of Ca and Ba currents.

The fast time constants for inactivation of Ca currents mediated by CSk2 exhibited a U-shaped dependence on test potential, whereas those for Ba currents progressively decreased with increasing test potential (Fig. 4 *D*). The time constants for inactivation of Ca currents were similar for CSk2 and α_{1C} currents of comparable densities (Table I). These results demonstrate that chimera CSk2 undergoes Ca-dependent inactivation. In marked contrast, the inactivation of Ba currents mediated by CSk2 was dramatically slowed (Fig. 4 *A*), with the fast time constants for inactivation being

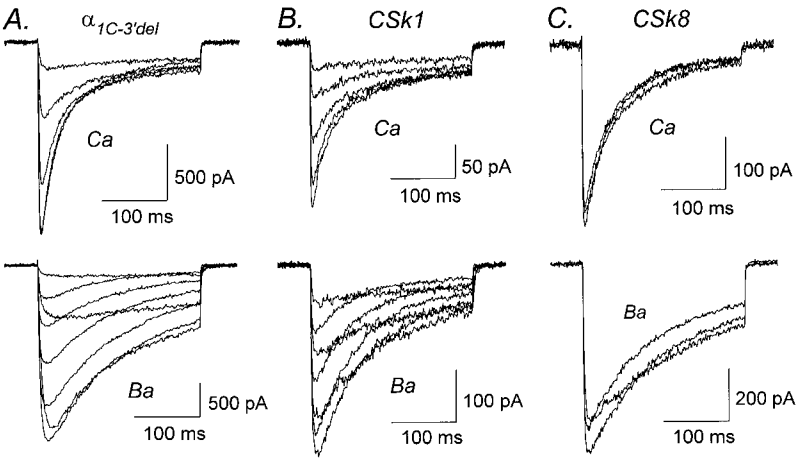

FIGURE 3. Ca-dependent inactivation is normal in $\alpha_{1C-3'del}$, CSk1, and CSk8. (*A*) Representative Ca (*top*) and Ba (*bottom*) currents mediated by $\alpha_{1C-3'del}$, a deletion mutant of α_{1C} lacking amino acid residues 1813–2166 from the COOH terminus. Test pulses from 0 to +40 mV (Ca) and −10 to +60 mV (Ba). Files 95929002, 95929006. C = 42 pF. R_S = 3.8 MΩ. (*B*) Representative Ca and Ba currents mediated by CSk1, a chimera in which the NH_2 terminus of α_{1C} was replaced by the corresponding region from α_{1S}. Test pulses from 0 to +40 mV (Ca) and 0 to +60 mV (Ba). Files 95D01016, 95D01018. C = 21 pF. R_S = 6.3 MΩ. (*C*) Representative Ca and Ba currents mediated by chimera CSk8, in which the III–IV loop of α_{1C} was replaced by the corresponding region from α_{1S}. Test pulses from +30 to +50 mV (Ca) and +20 to +40 mV (Ba). Files 96118045, 96118053. C = 15 pF. R_S = 4.9 MΩ. Experiments summarized in this figure were done using the TEACl-based external solution.

approximately threefold larger than for α_{1C} (Table I). If the fast phase of Ba current inactivation primarily reflects an ion-dependent process as proposed by Ferreira et al. (1997), then the slower inactivation of CSk2 may indicate that Ba is less effective in triggering ion-dependent inactivation when the I–II loop has skeletal muscle as opposed to cardiac sequence. Such an interpretation would imply that the I–II loop of α_{1C} has a functional role in Ca-dependent inactivation if Ba- and Ca-dependent inactivation are equivalent. It is also possible that the process of voltage-dependent inactivation is affected somewhat by replacement of the I–II loop region.

We have previously demonstrated that the II–III loop of α_{1S} performs a critical function in skeletal muscle–type excitation–contraction coupling (Tanabe et al., 1990*b*), perhaps by interacting directly with the ryanodine receptor. The II–III loops of α_{1C} and α_{1S} also contain numerous (35 and 27, respectively) negatively charged aspartate or glutamate residues that could potentially be involved in Ca coordination (Fujita et al., 1993). In addition, the II–III loop of α_{1S} contains a consensus site for phosphorylation by PKA (Tanabe et al., 1987), whereas the II–III loop of α_{1C} lacks predicted PKA sites (Mikami et al., 1989). To test whether the II–III loop of α_{1C} performs a unique function in Ca-depen-

TABLE I

Data from HEK293 Cells Cotransfected with Expression Plasmids Encoding α_1, $\alpha_2\delta_a$, and β_{1a} Ca Channel Subunits

α_1 construct	Ca current density	Fast tau I_{Ca}	Fast tau I_{Ba}	External solution
	pA/pF	*ms*	*ms*	
α_{1C}	−56 ± 9 (17)	17 ± 2 (14)	88 ± 8 (7)	TEAC1
α_{1C}	−17 ± 3 (7)	38 ± 6 (7)	—	TEAC1
$\alpha_{1C-3'del}$	−68 ± 21 (7)	20 ± 4 (8)	93 ± 21 (6)	TEAC1
CSk1	−28 ± 5 (12)	20 ± 1 (11)	57 ± 11 (6)	TEAC1
CSk2	−28 ± 11 (8)	35 ± 4 (9)	295 ± 38 (8)	TEAC1
CSk2	−20 ± 7 (5)	51 ± 8 (5)	467 ± 107 (4)	NaCl
CSk3	−23 ± 6 (9)	31 ± 5 (9)	129 ± 13 (4)	TEAC1
CSk3	−45 ± 9 (6)	38 ± 5 (6)	106 ± 22 (3)	NaCl
CSk4	−16 ± 3 (10)	70 ± 4 (5)	75 ± 5 (5)	TEAC1
CSk4	−13 ± 5 (4)	82 ± 15 (4)	80 ± 10 (4)	NaCl
CSk5	−51 ± 12 (8)	32 ± 4 (10)	97 ± 9 (8)	TEAC1
CSk5	−17 ± 6 (5)	76 ± 7 (5)	111 ± 6 (7)	NaCl
CSk8	−51 ± 12 (8)	23 ± 4 (8)	110 ± 10 (7)	TEAC1

The external solution was based upon TEAC1 or NaCl (see MATERIALS AND METHODS for compositions). Time constants for inactivation were derived by fitting maximal Ca or Ba currents (i.e., at the peak of the I–V relationship) with one or two exponential functions. Only the fast time constants (fast tau) were analyzed. Currents were evoked by test pulses of 250 or 500 ms, or 1.25 or 5 s, as dictated by the inactivation rate. Mean ± SEM, with the number of cells (*n*) in parentheses.

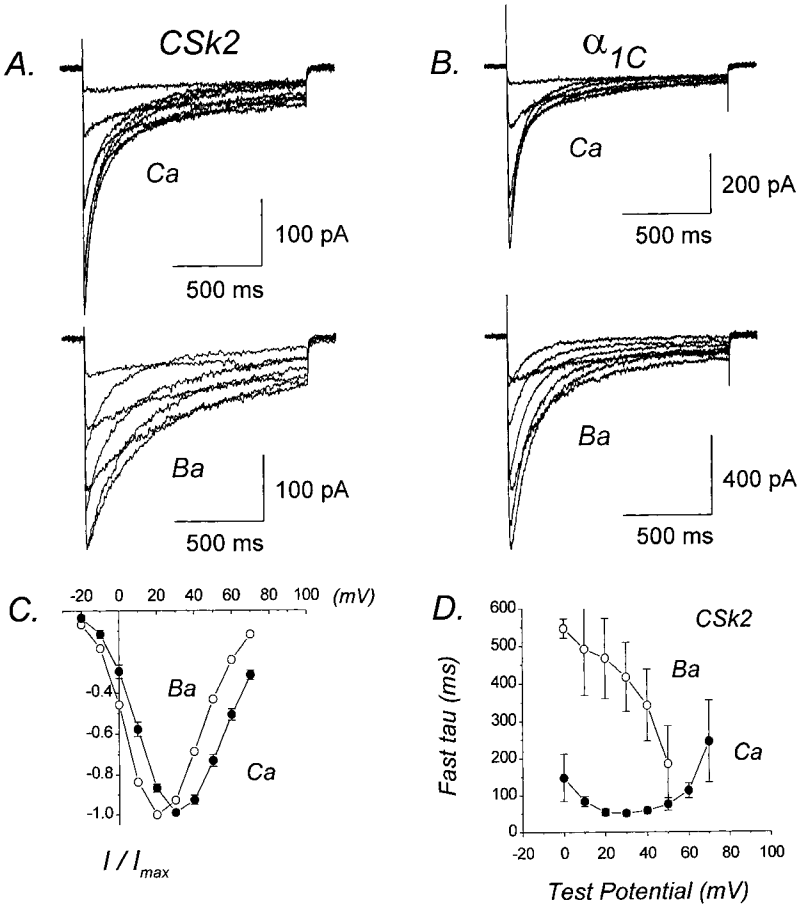

FIGURE 4. CSk2 retains Ca-dependent inactivation, but Ba current inactivation is dramatically slowed. (*A*) Representative Ca and Ba currents mediated by CSk2. Test pulses from −10 to +60 mV (Ca) and −10 to +50 mV (Ba). Files 97428010, 97428014. $C = 17$ pF. $R_S = 2.2$ MΩ. (*B*) Representative Ca and Ba currents mediated by α_{1C}. Test pulses from −10 to +40 mV (Ca) and −10 to +50 mV (Ba). Files 97502005, 97502012. $C = 31$ pF. $R_S = 2.3$ MΩ. (*C*) *I–V* relations for CSk2 currents. Plotted points represent the mean (±SEM) of 4–10 different cells. (*D*) Voltage dependence of fast time constants for inactivation of CSk2. Plotted points represent mean (±SEM) of four to five different cells. Experiments summarized in this figure were done using the NaCl-based external solution.

dent inactivation, we expressed chimera CSk3 in which the II–III loop of α_{1C} was replaced by its counterpart from α_{1S} (Fig. 2). CSk3 undergoes Ca-dependent inactivation because Ca currents inactivated much faster than Ba currents (Fig. 5). Furthermore, both Ca and Ba currents exhibited two distinct components of inactivation. The fast time constants for inactivation of Ca currents exhibited a U-shaped dependence on test potential; in contrast, such a relationship was not apparent for Ba currents (Fig. 5 *D*). Similar to the results obtained for CSk2, the fast component of Ba current inactivation was slightly slower for CSk3 than for α_{1C} (Table I), raising the possibility that the II–III loop may perform a functional role in Ca- or voltage-dependent inactivation.

Several previous studies have identified the COOH terminus of α_{1C} as an important structural determinant of Ca-dependent inactivation (de Leon et al., 1995; Soldatov et al., 1997; Zhou et al., 1997). To obtain further information regarding this issue, we expressed chimera CSk4 in which the distal 80% of the COOH terminus of α_{1C} was replaced by the corresponding region from α_{1S} (Fig. 2). In contrast to the other chimeras examined, Ca and Ba currents mediated by CSk4 inactivated at equivalent rates (Fig. 6, *A* and *B*). Both Ca and Ba currents exhibited two distinct components of inactivation. However, there was no difference between the fast time constants for inactivation of Ca currents and those for Ba currents over a wide range of test potentials and time constants for inactivation of Ca currents did not have a U-shaped dependence upon test potential (Fig. 6 *D*). These results demonstrate that CSk4 lacks Ca-dependent inactivation. As shown in Table I, the fast time constants for inactivation of Ca currents were three- to fourfold larger for CSk4 than for α_{1C}. This slow inactivation of Ca currents cannot be explained by low expression of CSk4, because inactivation was also slow compared with low density currents mediated by α_{1C} (Table I). Interestingly, the fast time constants for inactivation of Ba currents were not different between CSk4 and α_{1C}, suggesting that the fast component of Ba current inactivation is unaltered in CSk4.

The results obtained with $\alpha_{1C\text{-}3'\text{del}}$ (Fig. 3) confirm that a large segment of the distal COOH terminus is not required for Ca-dependent inactivation (Zong et al., 1994; de Leon et al., 1995). In contrast, the results obtained with CSk4 (Fig. 6) suggest that the COOH terminus of α_{1S} can somehow prevent Ca-dependent inactivation. A comparison of the COOH termini of α_{1C} and α_{1S} (Fig. 7) reveals substantial conservation of their sequences for ~200 amino acids after the end of the last predicted transmembrane segment (IVS6). Beyond

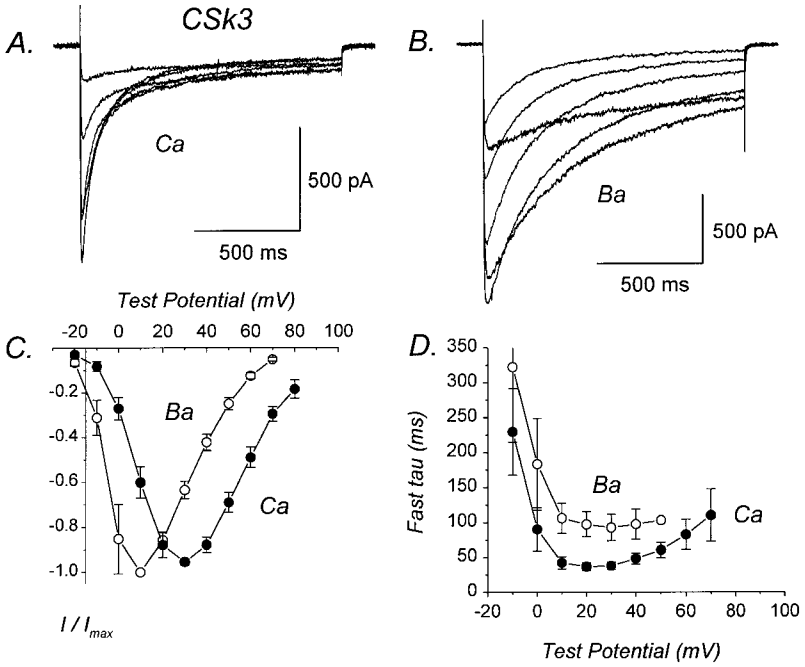

FIGURE 5. CSk3 exhibits Ca-dependent inactivation. (*A*) Representative Ca currents mediated by CSk3. Test pulses from −10 to +40 mV. File 97512062. $C = 41$ pF. $R_S = 4.0$ MΩ. (*B*) Representative Ba currents mediated by CSk3. Test pulses from −10 to +40 mV. File 97512067. Same cell as in *A*. (*C*) *I–V* relations for CSk3 currents. Plotted points represent the mean (±SEM) of three to eight different cells. (*D*) Voltage dependence of fast time constants for inactivation of CSk3. Plotted points represent mean (±SEM) of three to six different cells. Experiments summarized in this figure were done using the NaCl-based external solution.

this point, however, the COOH termini of α_{1C} and α_{1S} diverge significantly. To test whether the distal, nonconserved portion of the COOH terminus from α_{1S} could be responsible for the inability of CSk4 to undergo Ca-dependent inactivation, we constructed chimera CSk5 (Fig. 2). This construct is a truncation mutant of CSk4 in which the final 211 amino acids of the COOH terminus have been deleted, effectively removing the majority of the sequence that is not conserved between α_{1C} and α_{1S} (Fig. 7).

CSk5 undergoes Ca-dependent inactivation, as evidenced by the significantly faster inactivation of Ca than of Ba currents (Fig. 8, *A* and *B*; Table I). Two distinct components of inactivation were present in both Ca and Ba currents mediated by CSk5. The fast time constants for inactivation of Ca currents exhibited a U-shaped voltage dependence, whereas those for Ba currents did not (Fig. 8 *D*). At test potentials of +10, +20, and +30 mV, the fast time constants for inactivation of Ca currents were significantly smaller than for Ba currents (Fig. 8 *D*). The fast component of Ca current inactivation was slower for CSk5 than for α_{1C}, suggesting that Ca-dependent inactivation proceeds at a slower rate than in α_{1C}. As was found for CSk4, the fast

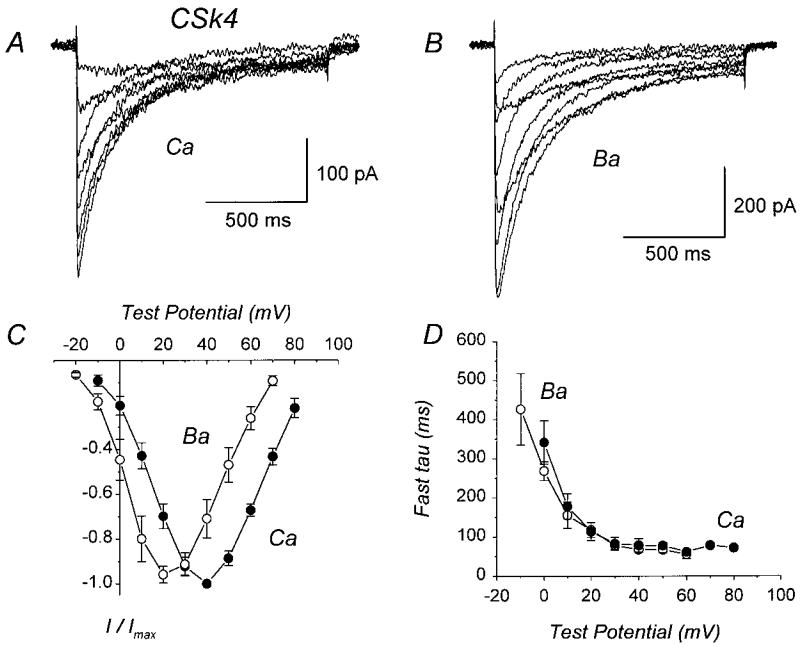

FIGURE 6. CSk4 lacks Ca-dependent inactivation. (*A*) Representative Ca currents mediated by CSk4, in which the distal 80% of the COOH terminus of α_{1C} has been replaced by the corresponding region from α_{1S}. File 97501003. $C = 26$ pF. $R_S = 3.6$ MΩ. (*B*) Representative Ba currents mediated by CSk4. File 97501008. Same cell as in *A*. For the illustrated currents, inactivation appears to be slightly slower for Ba than for Ca currents, but this is only apparent: the Ba currents are larger and therefore less contaminated by outward currents. (*C*) *I–V* relations for CSk4 currents. Each point represents the mean (±SEM) of four different cells. (*D*) Voltage dependence of fast time constants for inactivation of CSk4 currents. Each point represents the mean (±SEM) of four different cells. Experiments summarized in this figure were done using the NaCl-based external solution.

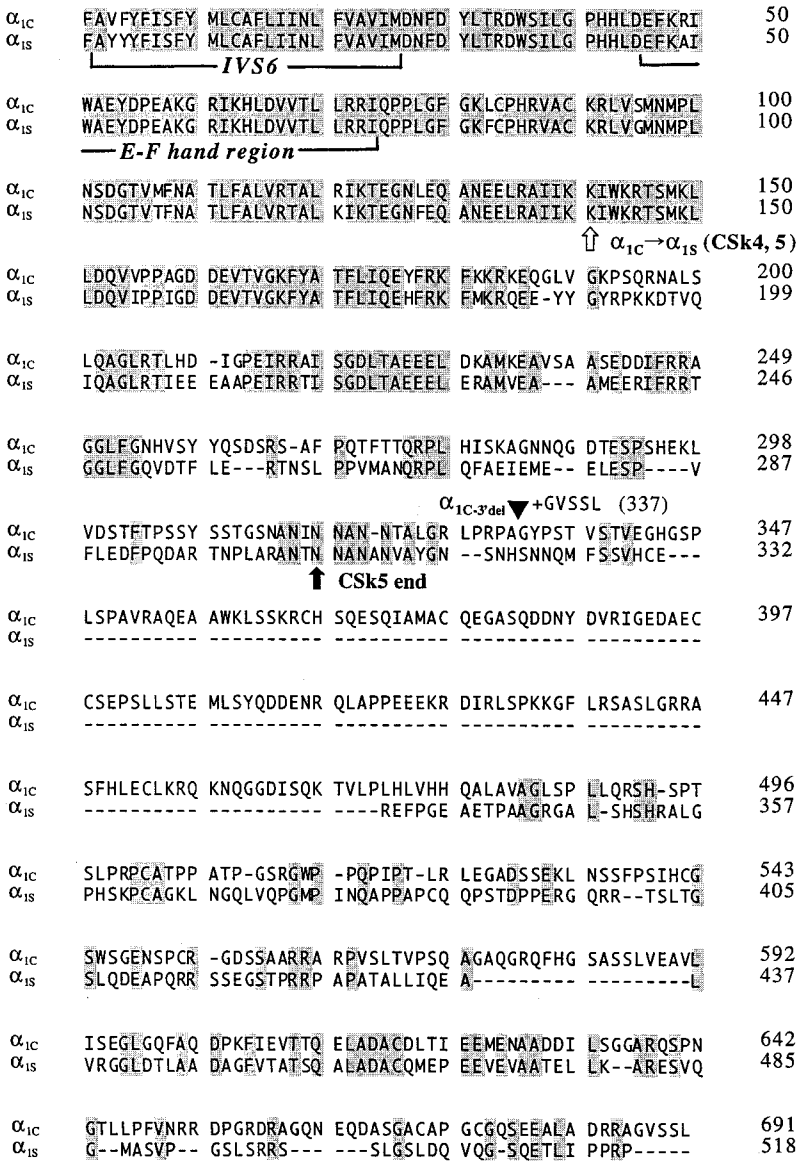

FIGURE 7. Sequence alignment of the COOH-terminal regions of the rabbit cardiac α_{1C} (Mikami et al., 1989) and rabbit skeletal muscle α_{1S} subunits (Tanabe et al., 1987). The sequences begin just before the last predicted transmembrane segment (S6) of domain IV (*first bracket*). The putative EF hand motif is indicated (*second bracket*), as is the junctional site within CSk4 and CSk5 where the sequence changes from α_{1C} to α_{1S} (*white arrow*). The termination of mutant $\alpha_{1C-3'del}$ is indicated by a filled triangle; this construct retains the final five residues (GVSSL) of the wild-type COOH terminus. The termination point of chimera CSk5 is indicated (*black arrow*). Shaded amino acids are identical between α_{1C} and α_{1S}; dashes indicate gaps in the alignment.

time constant for inactivation of Ba currents was not different between CSk5 and α_{1C} (Table I).

DISCUSSION

The goal of the present study was to gain new insights into the molecular mechanism of Ca-dependent inactivation by identifying structural regions of α_{1C} involved in this phenomenon. Toward this end, we compared inactivation of Ca and Ba currents mediated by chimeras constructed between the cardiac α_{1C}, which exhibits prominent Ca-dependent inactivation, and the skeletal muscle α_{1S}, which lacks this property (Donaldson and Beam, 1983; Beam and Knudson, 1988).

The protein sequence homology between α_{1C} and α_{1S} is ~66%, with the majority of the amino acid differences occurring within the major cytoplasmic domains (Mikami et al., 1989). For example, the NH_2 terminus of α_{1C} contains 154 amino acids, whereas that of α_{1S} contains only 50 amino acids. At the other extreme, the III–IV loops of α_{1C} and α_{1S} are highly conserved, both being 53 amino acids in length with only 7 amino acid differences. Our results with chimeras CSk1 and CSk8 suggest that neither the NH_2 terminus nor the III–IV loop of α_{1C} performs an essential function in Ca-dependent inactivation, because Ca and Ba currents mediated by these constructs are nearly identical to those mediated by α_{1C} (Fig. 3). However, because the III–IV loop is so highly conserved between α_{1C} and α_{1S}, this region may function interchangeably in Ca-dependent inactivation.

We have also found that inactivation of Ba current is dramatically slowed for chimera CSk2, in which the I–II loop of α_{1C} is replaced by the corresponding region

from α_{1S} (Fig. 4; Table I). This result is consistent with the relative inactivation rates of α_{1C} and α_{1S}, when these two different L-type Ca channels are expressed in dysgenic myotubes (Tanabe et al., 1990*a*). Our results with CSk2 are also consistent with the finding of Page et al. (1997) that inactivation was slowed by replacing the entire I–II loop of the relatively fast inactivating α_{1E} with the I–II loop from the more slowly inactivating α_{1B}. It is also interesting to compare our results for CSk2 with those of Zhang et al. (1994), who identified transmembrane segment IS6 and its immediately flanking regions as important determinants of voltage-dependent inactivation. A comparison of the I–II loops of α_{1C} and α_{1S} reveals that most amino acid differences occur within the COOH-terminal half, whereas the NH_2-terminal half of the I–II loop is comparatively well conserved (Mikami et al., 1989). The slowed inactivation of CSk2 may thus indicate an important role for the COOH-terminal portion of the I–II loop in Ca channel inactivation. However, because the NH_2-terminal portion of the I–II loop contains an interaction site for the Ca channel β subunit (Pragnell et al., 1994), and different β subunit isoforms can modulate the rate of Ca channel inactivation (Hullin et al., 1992), it is also possible that altered interactions between CSk2 and the β subunit are partially responsible for its slower inactivation. No consensus sites for phosphorylation by PKA or PKC are present within the I–II loop of either α_{1C} or α_{1S}; thus, it seems unlikely that differential phosphorylation could account for the slower inactivation of CSk2.

Ca-dependent inactivation is usually defined as the faster inactivation of Ca than Ba currents and by a U-shaped voltage dependence of the time constants for Ca current inactivation. Inactivation of Ba currents is usually assumed to proceed through a voltage-dependent process. However, Ferreira et al. (1997) have recently demonstrated that Ba can trigger the ion-dependent inactivation of α_{1C}. They found that Ba currents inactivate with two distinct components, and that the rate and extent of the fast component parallels Ba influx, whereas the rate and extent of the slow component parallels immobilization of gating charge (Ferreira et al., 1997). If the fast component of Ba current inactivation measured in our experiments reflects an ion-dependent process, then this process is significantly slowed in chimera CSk2, and to a lesser extent in chimera CSk3. In this view, our results with CSk2 suggest that the I–II loop of α_{1C} may be an important structural determinant of ion- rather than voltage-dependent inactivation. Such inactivation could be triggered (physiologically) by Ca or (experimentally) by Ba binding to the I–II and II–III loops of α_{1C} but not to the homologous regions of α_{1S}. If this interpretation is correct, then the I–II and II–III loops of α_{1C} are structural determinants of Ca-dependent inactivation.

We have demonstrated that CSk4, a chimera in which the COOH terminus of α_{1C} has been replaced by the corresponding region from α_{1S}, lacks Ca-dependent inactivation. This result is not an artifact stemming from low channel expression because the current density in cells expressing CSk4 was not significantly different from that in cells expressing CSk2 or CSk3 (Table I), which both displayed prominent Ca-dependent inactivation. Furthermore, Ca-dependent inactivation was

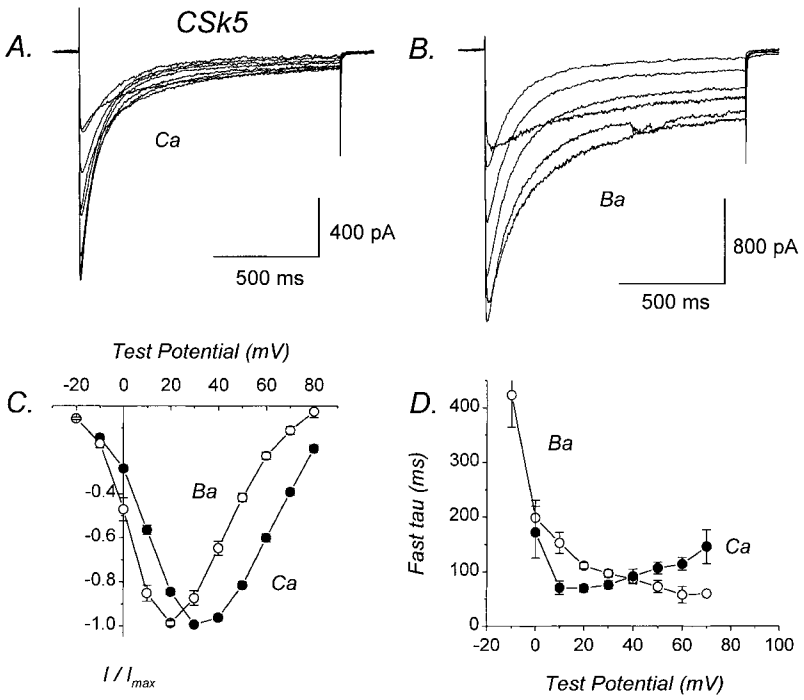

FIGURE 8. Ca-dependent inactivation is restored in CSk5. (*A*) Representative Ca currents mediated by CSk5, which is identical to CSk4 except that the nonconserved region (211 amino acids) has been deleted from the end of the COOH terminus. File 97522014. C = 43 pF. R_S = 3.0 MΩ. (*B*) Representative Ba currents mediated by CSk5. File 97522021. Same cell as in *A*. (*C*) *I–V* relations for CSk5 currents. Each plotted point represents the mean (±SEM) of eight different cells. (*D*) Voltage dependence of fast time constants for inactivation of CSk5 currents. Each plotted point represents the mean (±SEM) of five to six different cells. Experiments summarized in this figure were done using the NaCl-based external solution.

absent even from relatively high density CSk4 currents (not shown), whereas it was present in relatively low density α_{1C}, CSk1, CSk2, or CSk3 currents (e.g., Figs. 3 and 4). The lack of Ca-dependent inactivation by CSk4 may explain why this property is not exhibited by the skeletal muscle L-type Ca channel. In this regard, it would be interesting to know whether the property of Ca-dependent inactivation was gained or retained by α_{1C} during the course of Ca channel evolution. A recent report that the neuronal α_{1D} (an L-type Ca channel) also exhibits Ca-dependent inactivation (Hans et al., 1997) suggests that this property has been retained by α_{1C} and α_{1D} and lost by α_{1S}.

The mechanism of Ca-dependent inactivation is not known, but it has been proposed that a putative EF hand motif located within the proximal COOH terminus of α_{1C} functions as the essential Ca-binding site responsible for triggering Ca-dependent inactivation (de Leon et al., 1995). However, recent evidence from other laboratories suggests that the putative EF hand motif is not important in the mechanism of Ca-dependent inactivation. Thus, transfer of the putative EF hand from α_{1C} into α_{1E} fails to confer Ca-dependent inactivation and, conversely, transfer of the EF hand from α_{1E} into α_{1C} fails to disrupt it (Zhou et al., 1997). Additionally, Ca-dependent inactivation is not abolished by point mutations within α_{1C} that eliminate the Ca-coordination site from the putative EF hand motif but leave the remainder of the COOH terminus intact (Zhou et al., 1997). These results strongly suggest that the exact site or sites of Ca binding remain to be identified.

Because CSk5 undergoes Ca-dependent inactivation (Fig. 8), it is reasonable to suppose that it contains one or more Ca binding sites. It follows that CSk4 contains the same site or sites, because it encompasses the entire sequence of CSk5 (Fig. 7). However, CSk4 lacks Ca-dependent inactivation (Fig. 6), which leads to the conclusion that Ca binding to the α_1 subunit is only a prerequisite for Ca-dependent inactivation and is by itself insufficient. Presumably, Ca-dependent inactivation requires both Ca binding and a subsequent conformational shift of the channel protein(s).

Perhaps the most significant result of the present study is that Ca-dependent inactivation was restored in chimera CSk5 by deletion of the nonconserved, distal region of the COOH terminus present in CSk4 (Figs. 2 and 8). The COOH terminus of CSk5 is similar in length and composition to that of $\alpha_{1C-3'del}$ (Fig. 7). The behavior of $\alpha_{1C-3'del}$ clearly demonstrates that the most distal ~350 amino acids of the COOH terminus of α_{1C} are not required for Ca channel inactivation (Fig. 3 *A*; Zong et al., 1994; de Leon et al., 1995). In contrast, Ca-dependent inactivation is conferred upon the α_{1E} backbone by replacing a 134–amino acid segment immediately downstream from the putative EF hand region with the homologous 142–amino acid segment from α_{1C} (Zhou et al., 1997). Furthermore, Ca-dependent inactivation is profoundly influenced by splice variations within the proximal COOH terminus of α_{1C} immediately downstream from the putative EF hand region (Soldatov et al., 1997). Our results with CSk5 suggests that the proximal COOH termini of α_{1C} and α_{1S} (which are mostly conserved) can function interchangeably in Ca-dependent inactivation. When considered altogether, our results and those of other studies indicate that the proximal COOH terminus downstream from the putative EF hand region is an important structural determinant of Ca-dependent inactivation. However, de Leon et al. (1995) showed that Ca-dependent inactivation was only partially conferred upon the neuronal α_{1E} subunit by replacing its entire COOH terminus with 217 amino acids from the corresponding region of α_{1C}. Thus, while the proximal COOH terminus appears to be important for Ca-dependent inactivation, the participation of additional channel regions may also be required.

Our findings that CSk4 lacks Ca-dependent inactivation, whereas this property is restored in CSk5, suggests that the distal COOH terminus of α_{1S} (which is not well conserved between α_{1C} and α_{1S}) can somehow block Ca-dependent inactivation. The mechanism by which this block occurs is, at present, purely speculative. However, because ion channels appear to associate with many other proteins in vivo (Sheng and Kim, 1996), it seems plausible that CSk4 might be tethered through its distal COOH terminus to other proteins (such as ryanodine receptors, the cytoskeleton, kinases, phosphatases, or other ion channels), and that such interactions might prevent the conformational shift underlying Ca-dependent inactivation.

We thank two anonymous reviewers for constructive criticisms. We also thank C. Adams and Drs. N. Artemyev, K. Melliti, and U. Meza for helpful comments on the manuscript.

B. Adams was supported by a Grant-In-Aid from the American Health Association (Iowa Affiliate), a research grant from the Muscular Dystrophy Association, and grant NS-34422 from the National Institutes of Health. T. Tanabe was supported by the Ministry of Education, Science and Culture of Japan and Howard Hughes Medical Institute.

Original version received 6 March 1997 and accepted version received 15 July 1997.

REFERENCES

Adams, B., and T. Tanabe. 1996. Calcium-dependent inactivation of heterologously expressed cardiac L-type calcium channel. *Biophys. J.* 70:238*a.* (Abstr.)

Beam, K.G., and C.M. Knudson. 1988. Calcium currents in embryonic and neonatal mammalian skeletal muscle. *J. Gen. Physiol.* 91: 781–798.

Beam, K.G., B.A. Adams, T. Niidome, S. Numa, and T. Tanabe. 1992. Function of a truncated dihydropyridine receptor as both voltage sensor and calcium channel. *Nature (Lond.).* 360:169–171.

Boyett, M.R., S.M. Harrison, N.C. Janvier, S.O. McMorn, J.M. Owen, and Z. Shui. 1996. A list of vertebrate cardiac ionic currents: nomenclature, properties, function and cloned equivalents. *Cardiovasc. Res.* 32:455–481.

de Leon, M., Y. Wang, L. Jones, E. Perez-Reyes, X.Y. Wei, T.W. Soong, T.P. Snutch, and D.T. Yue. 1995. Essential Ca^{2+}-binding motif for Ca^{2+}-sensitive inactivation of L-type Ca^{2+} channels. *Science (Wash. DC).* 270:1502–1506.

Donaldson, P.L., and K.G. Beam. 1983. Calcium currents in a fast-twitch skeletal muscle of the rat. *J. Gen. Physiol.* 83:449–468.

Ferreira, G., J. Yi, E. Rios, and R. Shirokov. 1997. Ion-dependent inactivation of barium current through L-type calcium channels. *J. Gen. Physiol.* 109:449–461.

Fujita, Y., M. Mynlieff, R.T. Dirksen, M.-S. Kim, T. Niidome, J. Nakai, T. Friedrich, N. Iwabe, T. Miyata, T. Furuichi, et al. 1993. Primary structure and functional expression of the ω-conotoxin-sensitive N-type calcium channel from rabbit brain. *Neuron.* 10:585–598.

Haack, J.A., and R.L. Rosenberg. 1994. Calcium-dependent inactivation of L-type calcium channels in planar lipid bilayers. *Biophys. J.* 66:1051–1060.

Hadley, R.W., and W.J. Lederer. 1991. Ca^{2+} and voltage inactivate Ca^{2+} channels in guinea-pig ventricular myocytes through independent mechanisms. *J. Physiol. (Oxf.).* 444:257–268.

Hamill, O.P., A. Marty, E. Neher, B. Sakmann, and F.J. Sigworth. 1981. Improved patch-clamp techniques for high-resolution current recording from cells and cell-free membrane patches. *Pflüg. Arch. Eur. J. Physiol.* 391:85–100.

Hans, M., A. Urrutia, P. Brust, A. Nesterova, A.I. Sacaan, M. Harpold, and K. Stauderman. 1997. Biophysical and pharmacological properties of human neuronal $\alpha_{1D}\alpha_{2b}\delta\beta_{3a}$ Ca^{2+} channels stably expressed in HEK293 cells. *Biophys. J.* 72:*A*146. (Abstr.)

Hofmann, F., M. Biel, and V. Flockerzi. 1994. Molecular basis for Ca^{2+} channel diversity. *Annu. Rev. Neurosci.* 17:399–418.

Hullin, R., D. Singer-Lahat, M. Freichel, M. Biel, N. Dascal, F. Hofmann, and V. Flockerzi. 1992. Calcium channel β subunit heterogeneity: functional expression of cloned cDNA from heart, aorta and brain. *EMBO (Eur. Mol. Biol. Organ.) J.* 11:885–890.

Imredy, J.P., and D.T. Yue. 1994. Mechanism of Ca^{2+}-sensitive inactivation of L-type Ca^{2+} channels. *Neuron.* 12:1301–1318.

Jurman, M.E., L.M. Boland, Y. Liu, and G. Yellen. 1994. Visual identification of individual transfected cells for electrophysiology using antibody-coated beads. *Biotechniques.* 17: 876–881.

Mikami, A., K. Imoto, T. Tanabe, T. Niidome, Y. Mori, H. Takeshima, S. Narumiya, and S. Numa. 1989. Primary structure and functional expression of the cardiac dihydropyridine-sensitive calcium channel. *Nature (Lond.).* 340:230–233.

Mishina, M., T. Kurosaki, T. Tobimatsu, Y. Morimoto, M. Noda, T. Yamamoto, M. Terao, J. Lindstrom, T. Takahashi, M. Kuno, and S. Numa. 1984. Expression of functional acetylcholine receptor from cloned cDNAs. *Nature (Lond.).* 307:604–608.

Neely, A., R. Olcese, X. Wei, L. Birnbaumer, and E. Stefani. 1994. Ca^{2+}-dependent inactivation of a cloned cardiac Ca^{2+} channel α_1 subunit (α_{1C}) expressed in *Xenopus* oocytes. *Biophys. J.* 66:1895–1903.

Obejero-Paz, C.A., S.W. Jones, and A. Scarpa. 1991. Calcium currents in the A7r5 smooth muscle-derived cell line: increase in current and selective removal of voltage-dependent inactivation by intracellular trypsin. *J. Gen. Physiol.* 98:1127–1140.

Page, K.M., G.J. Stephens, N.S. Berrow, and A.C. Dolphin. 1997. The intracellular loop between domains I and II of the B-type calcium channel confers aspects of G-protein sensitivity to the E-type calcium channel. *J. Neurosci.* 17:1330–1338.

Perez-Garcia, M.T., T.J. Kamp, and E. Marbán. 1995. Functional properties of cardiac L-type calcium channels transiently expressed in HEK293 cells. Role of α_1 and β subunits. *J. Gen. Physiol.* 105:289–306.

Perez-Reyes, E., W. Yuan, X. Wei, and D.M. Bers. 1994. Regulation of the cloned L-type cardiac calcium channel by cyclic-AMP-dependent protein kinase. *FEBS Lett.* 342:119–123.

Pragnell, M., M. De Waard, Y. Mori, T. Tanabe, T.P. Snutch, and K.P. Campbell. 1994. Calcium channel β-subunit binds to a conserved motif in the I–II cytoplasmic linker of the α_1-subunit. *Nature (Lond.).* 368: 67–70.

Sheng, M., and E. Kim. 1996. Ion channel associated proteins. *Curr. Opin. Neurobiol.* 6:602–608.

Shirokov, R., R. Levis, N. Shirokova, and E. Rios. 1993. Ca^{2+}-dependent inactivation of cardiac L-type Ca^{2+} channels does not affect their voltage sensor. *J. Gen. Physiol.* 102:1005–1030.

Soldatov, N.M., R.D. Zühlke, A. Bouron, and H. Reuter. 1997. Molecular structures involved in L-type calcium channel inactivation. Role of the carboxyl-terminal region encoded by exons 40–42 in α_{1C} subunit in the kinetics and Ca^{2+} dependence of inactivation. *J. Biol. Chem.* 272:3560–3566.

Stühmer, W., F. Conti, H. Suzuki, X. Wang, M. Noda, N. Yahagi, H. Kubo, and S. Numa. 1989. Structural parts involved in activation and inactivation of the sodium channel. *Nature (Lond.).* 339:597–603.

Tanabe, T., A. Mikami, S. Numa, and K.G. Beam. 1990*a.* Cardiac-type excitation–contraction coupling in dysgenic skeletal muscle injected with cardiac dihydropyridine receptor cDNA. *Nature (Lond.).* 344:451–453.

Tanabe, T., K.G. Beam, B.A. Adams, T. Niidome, and S. Numa. 1990*b.* Regions of the skeletal muscle dihydropyridine receptor critical for excitation-contraction coupling. *Nature (Lond.).* 346: 567–569.

Tanabe, T., H. Takeshima, A. Mikami, V. Flockerzi, H. Takahashi, K. Kangawa, M. Kojima, H. Matsuo, T. Hirose, and S. Numa. 1987. Primary structure of the receptor for calcium channel blockers from skeletal muscle. *Nature (Lond.).* 328:313–318.

Tanabe, T., K.G. Beam, J.A. Powell, and S. Numa. 1988. Restoration of excitation-contraction coupling and slow calcium current in dysgenic muscle by dihydropyridine receptor complementary DNA. *Nature (Lond.).* 336:134–139.

Vassilev, P., T. Scheuer, and W.A. Catterall. 1988. Identification of an intracellular peptide segment involved in sodium channel inactivation. *Science (Wash. DC).* 241:1658–1661.

Zhang, J.-F., P.T. Ellinor, R.W. Aldrich, and R.W. Tsien. 1994. Molecular determinants of voltage-dependent inactivation in calcium channels. *Nature (Lond.).* 372:97–100.

Zhou, J.M., R. Olcese, N. Qin, F. Noceti, L. Birnbaumer, and E. Stefani. 1997. Feedback inhibition of Ca^{2+} channels by Ca^{2+} depends on a short sequence of the C terminus that does not include the Ca^{2+}-binding function of a motif with similarity to Ca^{2+}-binding domains. *Proc. Natl. Acad. Sci. USA.* 94:2301–2305.

Zong, S., J. Zhou, and T. Tanabe. 1994. Molecular determinants of calcium-dependent inactivation in cardiac L-type calcium channels. *Biochem. Biophys. Res. Commun.* 201:1117–1123.

Zong, X.G., and F. Hofmann. 1996. Ca^{2+}-dependent inactivation of the class C L-type Ca^{2+} channel is a property of the α1 subunit. *FEBS Lett.* 378:121–125.